Meteoritics & Planetary Science 37, 439–448 (2002)
Available online at http://www.uark.edu/meteor

Fall, classification and cosmogenic records of the Sabrum (LL6) chondrite

S. GHOSH[1], S. V. S. MURTY[2], P. N. SHUKLA[2], A. D. SHUKLA[2], R. R. MAHAJAN[2], N. BHANDARI[2*],
N. C. PANT[1], J. B. GHOSH[1] AND S. SHOME[1]

[1]Geological Survey of India, 27 J. L. Nehru Road, Calcutta 700 016, India
[2]Physical Research Laboratory, Navrangpura, Ahmedabad 380 009, India
*Correspondence author's e-mail address: bhandari@prl.ernet.in

(Received 2001 September 6; accepted in revised form 2001 December 7)

Abstract–The petrographic and chemical characteristics of a fresh Indian meteorite fall at Sabrum are described. Its mean mineral composition is defined by olivine ($Fa_{31.4}$), orthopyroxene ($Fs_{25.1}$,$Wo_{2.0}$), clinopyroxene ($Wo_{45}En_{45.6}Fs_{9.4}$) and plagioclase ($An_{10.6}Ab_{83.6}Or_{5.8}$). The meteorite shows moderate shock features, which indicate that it belongs to the S4 category. Based on mineralogical and chemical criteria the meteorite is classified as an LL6 brecciated veined chondrite. Several cosmogenic radioisotopes (^{46}Sc, ^{7}Be, ^{54}Mn, ^{22}Na and ^{26}Al), noble gas (He, Ne, Ar, Kr and Xe), nitrogen isotopes, and particle tracks density have been measured. Concentrations of cosmogenic ^{21}Ne and ^{38}Ar indicate that its cosmic-ray exposure age is 24.8 Ma. Small amounts of trapped Kr and Xe, consistent with petrologic class 5/6, are present. The track density in olivines is found to be $(1.3 \pm 0.3) \times 10^6$/cm^2. Activities of most of the short-lived isotopes are lower than those expected from solar cycle variation. ^{22}Na/^{26}Al (1.12 ± 0.02) is found to be significantly anomalous, being ~25% lower than expected from the Climax neutron monitor data. These results indicate that the cosmic-ray flux during the terminal segment of the meteoroid orbit was low. The activities of ^{26}Al and ^{60}Co and the track density indicate small meteoroid size with a radius ~15 cm.

FALL AND MORPHOLOGY

A single stone weighing ~1.5 kg fell on 1999 April 30, near Chautrishghat village in the Sabrum tehsil (23°05' N; 91°40' E) of South Tripura district, India. As reported in *The Telegraph*, Calcutta, dated 1999 May 3, people near a bathing pond heard a whistling sound followed by the fall of a dark object, which created a small pit on the ground. Based on this report, 478 g (~10.0 × 6.2 × 5.6 cm) of the stone was collected by the Geological Survey of India (GSI), Calcutta.

The piece examined by us consists of two faces partly covered with fusion crust and two fractured surfaces and appears to be a part of an ellipsoid (Fig. 1). The larger face representing the top of the ellipsoid is smooth, covered with indistinct radiating grooves and a few shallow regmaglypts. The larger fractured surface shows a brecciated greyish matrix which includes strongly integrated clasts of variable size, the largest being 1 × 0.5 cm. Chondrules appear to be well integrated with the matrix and are not easily distinguishable.

Fusion crust on the large convex face is dark brownish grey, 0.5 mm thick, having numerous polygonal shrinkage cracks. The matrix material in the cracks bears evidence of effervescence. Crudely defined radiating grooves and ribs are noticeable from the top of the partial ellipsoid towards the edges. The fusion crust on the smaller face at the ellipsoidal base is dark brown, both close-textured and scoriaceous and variable in thickness (0.5 to 1 mm). Scoriaceous texture, mainly along the margin, appears to be due to stagnation of flowage material.

PETROGRAPHY AND MINERAL CHEMISTRY

Megascopically Sabrum meteorite is an intensely brecciated and strongly recrystallised ordinary chondrite with no readily distinguishable chondrules or Fe-Ni metal specks. In polished thin sections, a few large (average 0.75 mm across) and plenty of small lithic clasts are seen in a dense, dark grey semi-translucent crystalline matrix (Fig. 2). Lithic clasts are mostly subangular to subrounded chondritic fragments with vestiges of various types of chondrules. Some of them could be identified as belonging to radial pyroxene (RP), porphyritic olivine (PO), barred olivine (BO), granular olivine (GO) and cryptocrystalline (C) types. In the clasts, chondrules and the adjacent matrix are much recrystallised and represent a coarse homogeneous aggregate mainly of olivine and orthopyroxene and minor secondary plagioclase and clinopyroxene (Fig. 3). Besides, there are a few droplet chondrules, mostly of devitrified glass in composition. Large troilite patches (average size

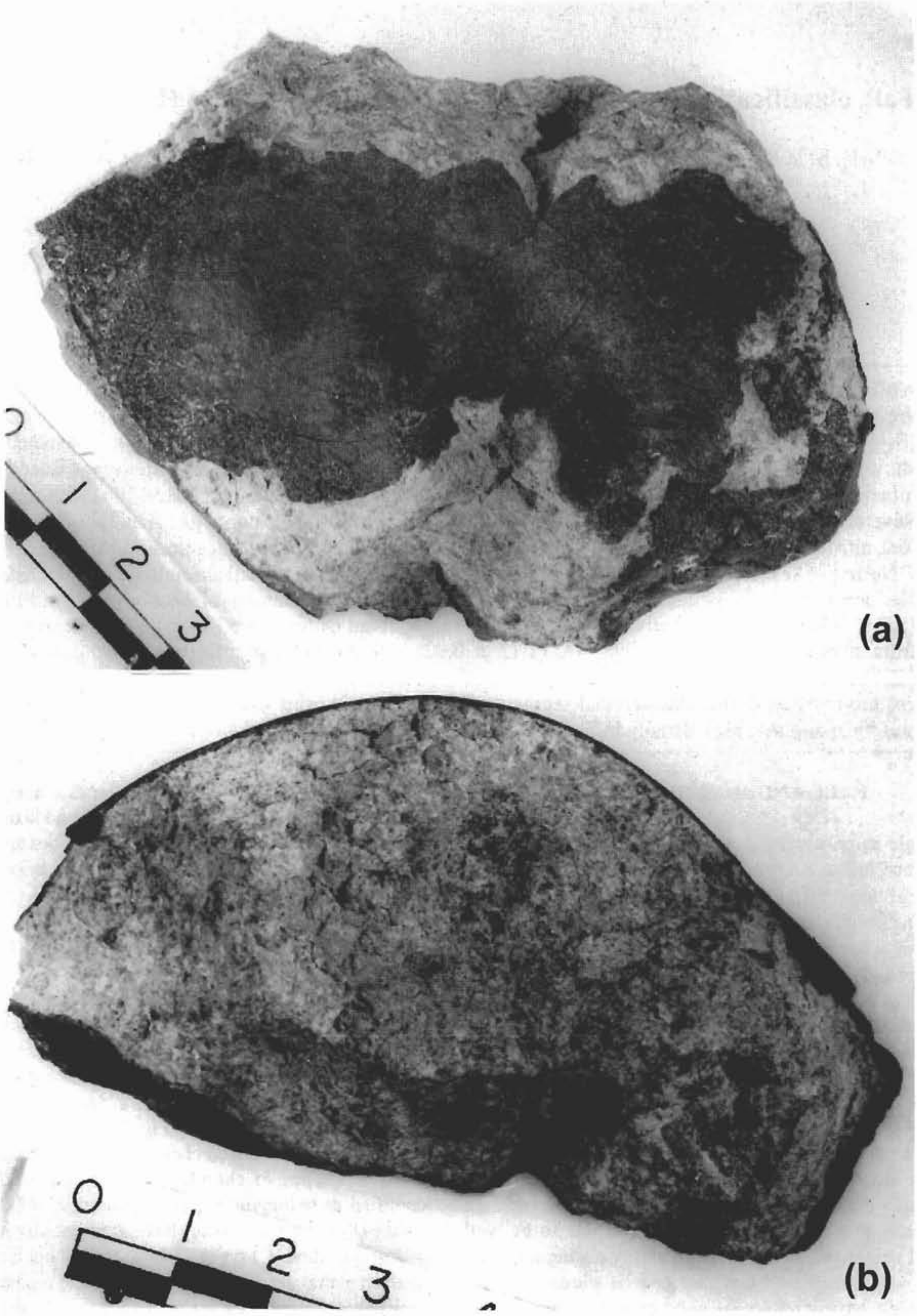

FIG. 1. Megascopic appearance of Sabrum chondrite showing smooth and scoriaceous surface textures with development of fine shrinkage cracks (scale bar in cm).

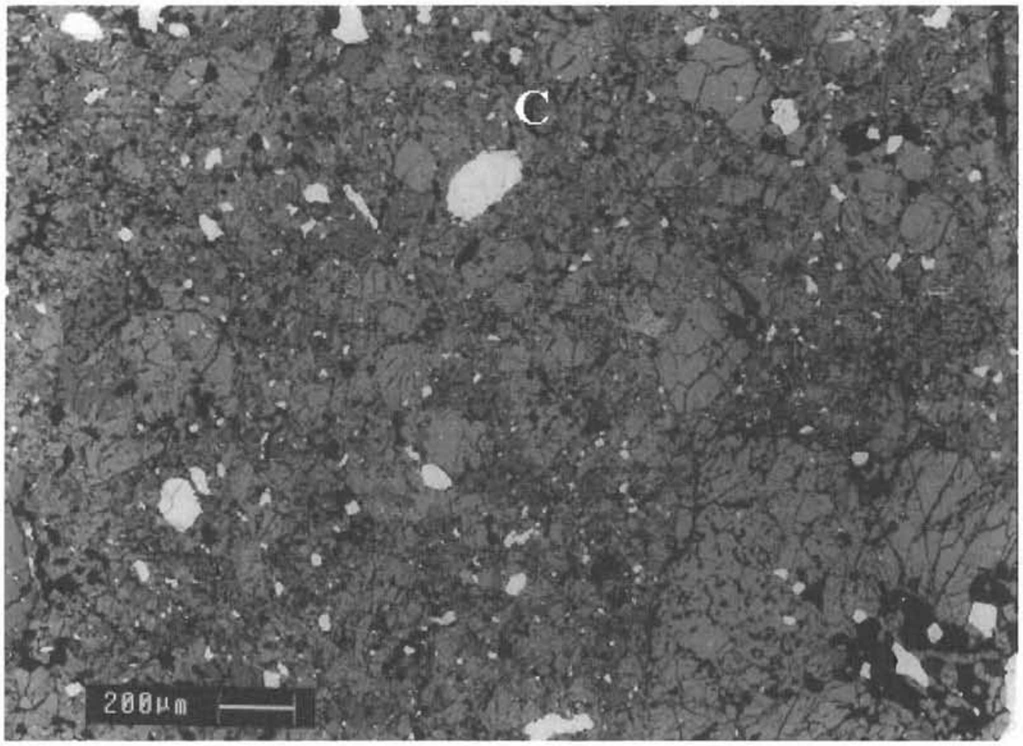

FIG. 2. Backscattered image of Sabrum chondrite showing intensely brecciated and moderate to highly recrystallised aggregate of lithic clasts, chondrule clasts (C) and mineral clasts.

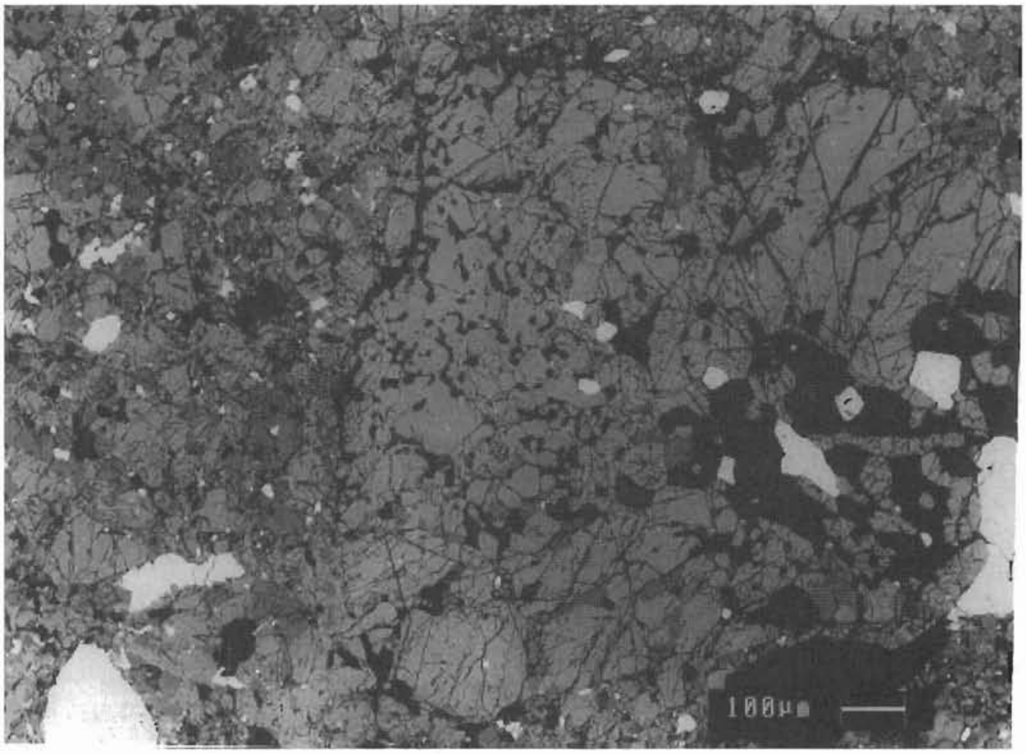

FIG. 3. Backscattered image of Sabrum chondrite showing an enlarged view of a lithic clast which is essentially made up of olivine, orthopyroxene, interstitial feldspar with troilite.

TABLE 1. Modal and mineral composition of the Sabrum chondrite.

Mineral	Modal abundance (vol%)	Mineral composition (number of observations)	Mean mineral composition
Olivine	55.9	$Fa_{30.4–32.2}$; CaO (wt%) 0.0–0.055 (27)	$Fa_{31.4}$
Orthopyroxene	20.6	$Fs_{23.9–26.0}$; $Wo_{1.5–2.4}$ (14)	$Fs_{25.1}Wo_{2.0}$
Plagioclase	10.9	$Ab_{81.3–84.9}$ $An_{10.3–11.1}$ $Or_{4.5–7.6}$ (9)	$Ab_{83.6}An_{10.6}Or_{5.8}$
Clinopyroxene	2.3	$Wo_{43.4–46.2}$ $En_{44.6–47.1}Fs_{8.1–10.8}$ (8)	$Wo_{45.0}En_{45.6}Fs_{9.4}$
Troilite	6.9	–	–
Fe-Ni metal	1.7	–	–
Chromite	1.7	–	–
Total	100.0		

0.7 × 0.5 mm) are common in addition to fine disseminated grains (~0.05 mm). Fe-Ni metal is much less abundant than troilite. Chromite is rare and coarse chromite grains (0.15 × 0.10 mm) are often fragmented. Shock veins are noticed across the chondrite on fine scale and coarse olivine grains show development of planar fractures and mosaicism. Following the shock facies classification (Stöffler *et al.*, 1991) Sabrum meteorite appears to be a brecciated veined ordinary chondrite, grade S4.

Different petrographic constituents of the Sabrum chondrite after optical microscopy were studied under scanning electron microscope–energy dispersive x-ray spectroscopy (SEM-EDX) employing a Leica 440 SEM. Backscattered images of essential minerals showing textural features were taken to facilitate the electron microprobe (EMPA) studies. The procedure and operating conditions are described in Ghosh *et al.* (2000). The modal mineralogical abundances based on automode EPMA analysis and the range and mean mineral compositions are given in Table 1.

The olivine and pyroxene compositions of Sabrum meteorite indicate LL group. Petrographic description given above indicates that Sabrum meteorite belongs to petrologic class 6 of Van Schmus and Wood (1967).

BULK CHEMISTRY

Interior chips (~4 g) representing the main mass were gently crushed and powdered in an agate mortar to provide the bulk sample. An aliquot (119.73 mg) from the bulk powder together with Dhajala (H 3.8) meteorite and U.S.G.S. diabase standard W-2 were treated with HF, HCl, $HClO_4$ and finally dissolved in dilute HNO_3 for inductively-coupled plasma atomic emission spectrometry (ICPAES) and atomic absorption spectroscopy (AAS) analysis for various elements (Al, Mg, Fe, Ti, Mn, Ba, Sr, Cu, Zn, V, Na and K). Further, two aliquots (~80 mg each) and a metallic fraction (25.08 mg) together with standards (Allende meteorite and U.S.G.S. basalt standard BCR-1) were irradiated in Dhruva reactor of BARC, Mumbai for instrumental neutron activation analysis (INAA). The irradiated samples were counted on a high-purity Ge detector (148 cm^3) located in a 10 cm thick lead shield following standard procedures (Laul, 1979; Shukla *et al.*, 1997). Thus, concentrations of Fe, Ni, Co, Ir, Os, Ca, Sc, Sm, Eu and Yb were determined. Typical errors of measurements and reproducibility were within ~5%. The data given in Table 2 represent the average concentration from various aliquots. Silicate, sulfide and metallic phases were separated from a 5 g piece of the meteorite and their chemical composition was also measured following the procedure described in Dasgupta *et al.* (1978) and Ghosh *et al.* (2000). The results are given in Table 3. The concentration reported in Tables 2 and 3 match reasonably well with each other except for Mn, K and Ti where the concentrations reported in Table 2, believed to be more accurate, are similar to those reported for LL chondrites (Kallemeyn *et al.*, 1989).

TABLE 2. Bulk chemical composition of the Sabrum chondrite.

Element	Concentration
Fe (%)	19.65
Mg (%)	14.65
Ca (%)	1.28
Al (%)	1.16
Ni (%)	0.99
Cr (ppm)	3313
Mn (ppm)	2673
Na (ppm)	6974
K (ppm)	817
Ti (ppm)	582
Co (ppm)	521
Cu (ppm)	79
Zn (ppm)	74
V (ppm)	25
Ba (ppm)	1.2
Sr (ppm)	9.7
Sc (ppm)	7.9
Sm (ppm)	0.21
Eu (ppm)	0.08
Yb (ppm)	0.20
Ir (ppb)	312
Os (ppb)	380

TABLE 3. Chemical composition of different phases in the Sabrum chondrite.

Composition	Weight (%)	Selected parameters	
Metallic phase			
Fe	2.04	Total Fe (%)	20.06
Ni	1.14	Fe_{metal}/Fe_{total}	0.102
Co	0.06	Fe/Si	1.05
Sulphide phase		Mg/Si	0.785
Fe	5.07	Al/Si	0.055
Ni	0.06	Ni/Fe_{metal}	0.59
Co	<0.01		
S	2.73		
Silicate and oxide phase			
SiO_2	40.90		
TiO_2	0.08		
Al_2O_3	2.00		
Cr_2O_3	0.48		
Fe_2O_3	Trace		
FeO	16.60		
MnO	0.45		
CaO	1.65		
MgO	24.98		
Na_2O	0.86		
K_2O	0.074		
P_2O_5	0.16		
Total	99.33		

Comparison of bulk chemical composition particularly the siderophile elements with various chondrite groups (Mason, 1971; Jarosewich, 1990) indicate that the meteorite belongs to the LL group. Position of Sabrum in the Urey–Craig diagram of iron in metal and sulfide phases *vs.* iron in oxide phases (Brearley and Jones, 1998) confirm this classification. Thus, the chemical and petrographical analyses suggest that the Sabrum meteorite belongs to the LL6 group of chondrites.

NOBLE GASES AND NITROGEN

A clean chip of the meteorite, part of which was used for chemical analysis, has been used for noble gas studies. The sample was wrapped in Al-foil and loaded into the extraction system of the noble gas mass spectrometer. All noble gases and nitrogen were analyzed by stepwise pyrolysis, after an initial combustion at 400 °C in 2 torr O_2 using standard procedures described earlier (Murty *et al.*, 1998; Bhandari *et al.*, 1998; Bonino *et al.*, 2001). The data reported here have been corrected for blanks, interferences and instrumental mass discrimination following the procedure of Murty *et al.* (1998). Blanks at all temperatures are <5% of the signal and have near atmospheric isotopic composition within errors. In the main sample, Ar could not be analyzed due to some technical reasons. The 400 °C fraction of Kr and Xe are found to be at blank levels. At 1000 and 1700 °C, due to small amounts of Kr and Xe present, as expected in a heavily metamorphosed meteorite of petrologic class 6, the fractions were combined for measurement. Even so, the low abundant isotopes of Kr (^{78}Kr, ^{80}Kr) and Xe (^{124}Xe, ^{126}Xe and ^{128}Xe) could not be measured with precision and here we report the composition for the more abundant isotopes of Kr and Xe.

The results of measurements of He, Ne and N are given in Table 4a, Ar in Table 4b and Kr and Xe in Table 4c. He and Ne are mostly dominated by cosmogenic and radiogenic (^{4}He) components, while in the case of Ar a small amount of trapped ^{36}Ar is also present. Though amounts of Kr and Xe are small, the isotopic composition show that a major proportion of them belong to the trapped component.

Cosmogenic Components and Exposure Ages

Using the end member compositions suggested by Eugster (1988), we have derived the cosmogenic ^{3}He, ^{21}Ne and ^{38}Ar. These are given in Table 5a. Cosmogenic $(^{22}Ne/^{21}Ne)_c$ has a value of 1.102 ± 0.002 as obtained by correcting the measured ratio for a small contribution from trapped Ne component. Using this value of $(^{22}Ne/^{21}Ne)_c$ and the chemical composition of Sabrum, we have derived the production rates for ^{3}He and ^{21}Ne following the procedure of Eugster (1988) and for ^{38}Ar by the method proposed by Marti and Graf (1992). The calculated cosmic-ray exposure ages T_3, T_{21}, and T_{38} based on the three rare gas isotopes are given in Table 5b. The exposure ages of 24.7 and 24.9 Ma based on ^{21}Ne and ^{38}Ar, respectively, are in agreement, and we adopt the average value of 24.8 Ma as the cosmic-ray exposure age of Sabrum. The observed value of $(^{21}Ne/^{38}Ar)_c = 8$ matches with the expected value for chondrites (Eugster, 1988), confirming that there has been no Ne or Ar losses. The ^{3}He exposure age of 20.1 Ma is, however, 18% lower than the ages based on ^{21}Ne and ^{38}Ar and indicate a partial ^{3}He loss.

Radiogenic Components and Gas Retention Ages

From the radiogenic ^{4}He and ^{40}Ar (Table 5a), we calculate a U,Th-^{4}He age of 3.21 Ga (using average U, Th values of LL chondrites; Wasson and Kallemeyn, 1988) and a K-Ar age of 4.42 Ga, using the measured K = 817 ppm (Table 5b). The lower ^{4}He age also points to a partial loss of radiogenic ^{4}He suggesting that the loss of He (both ^{3}He and ^{4}He) has occurred recently while the meteoroid was orbiting in interplanetary space. Assuming U content same as the average for LL chondrites (Wasson and Kallemeyn, 1988) and a Xe retention age of 4.5 Ga, only 0.5×10^{-12} cc STP/g of $^{136}Xe_f$ is expected, suggesting that almost all of the observed $^{136}Xe_f$ is produced by ^{244}Pu fission. The amounts of $^{136}Xe_f$ and $^{129}Xe_r$ are in the general range of values observed for LL6 chondrites (Eugster *et al.*, 1993).

TABLE 4a. Helium, Ne and N data for Sabrum (sample weight = 364.19 mg).

Temperature (°C)	^{4}He (10^{-8} ccSTP/g)	^{22}Ne (10^{-8} ccSTP/g)	N (ppm)	$^{3}He/^{4}He$	$^{20}Ne/^{22}Ne$	$^{21}Ne/^{22}Ne$	$\delta^{15}N$ (‰)
400	20.4	0.025	1.272	0.0252 ±0.0021	3.068 ±0.048	0.6801 ±0.0076	12.10 ±0.30
1000	1322	4.80	7.237	0.0235 ±0.0020	0.9423 ±0.0284	0.8911 ±0.0001	18.05 ±0.72
1700	29.0	4.68	0.527	0.0292 ±0.0025	0.8870 ±0.0010	0.9012 ±0.0005	43.38 ±0.30
Total	1371	9.50	9.036	0.0237 ±0.0020	0.9205 ±0.0145	0.8955 ±0.0003	18.69 ±0.63

Errors in concentrations are ±10%. Errors in isotopic composition represent 95% C. L.

TABLE 4b. Argon data for Sabrum (sample weight = 59.78 mg).

Temperature (°C)	^{36}Ar (10^{-8} ccSTP/g)	$^{38}Ar/^{36}Ar$	$^{40}Ar/^{36}Ar$
400	0.025	0.2391 ±0.0010	1450 ±12
1700	1.060	1.059 ±0.001	5679 ±52
Total	1.085	1.040 ±0.001	5580 ±51

TABLE 4c. Krypton and Xe data for Sabrum (sample weight = 364.19 mg).

^{84}Kr	^{132}Xe	^{82}Kr	^{83}Kr	^{86}Kr	^{129}Xe	^{130}Xe	^{131}Xe	^{134}Xe	^{136}Xe
(10^{-12} ccSTP/g)		(^{84}Kr = 100)			(^{132}Xe = 100)				
41.9	44.1	28.70 ±0.08	29.32 ±0.19	29.01 ±0.05	145.2 ±1.5	16.98 ±0.11	82.22 ±0.11	38.74 ±0.24	33.67 ±0.37

Trapped Component

Ne is almost purely cosmogenic. About 35% ^{36}Ar and >90% ^{84}Kr and ^{132}Xe are of trapped origin, the rest being cosmogenic. The elemental ratios $^{84}Kr/^{132}Xe$ = 0.9 and $^{36}Ar/^{132}Xe$ = 87 are in the range of values observed in ordinary chondrites (Swindle, 1988). The amounts of trapped gases (see Table 5a) are in the range expected for petrologic class 5/6 members of ordinary chondrites (Marti, 1967).

Nitrogen

Sabrum contains ~9 ppm N with $\delta^{15}N$ of 18.7‰. Major N release (80%) occurs at 1000 °C, and $\delta^{15}N$ monotonically increases, starting at 12.1‰ at 400 °C, going up to 43.4‰ at the melting step. These data indicate that cosmogenic N is released at higher temperatures. Using the total ^{21}Ne and the production ratio of $(^{15}N/^{21}Ne)_c = 4.5 \pm 0.5$ for LL chondrites of Sabrum size (Mathew and Murty, 1993), we correct the total $\delta^{15}N$ for cosmogenic contribution and obtain an average $\delta^{15}N = (11.5 \pm 0.5‰)$ for the trapped N component, which is close to the $\delta^{15}N$ of the 400 °C fraction. Similar $\delta^{15}N$ at 400 and 1000 °C suggests that Sabrum probably has a uniformly distributed trapped N component over which the cosmogenic signature has been superimposed. The amount of N present in Sabrum, however, is on the higher side for higher metamorphic class ordinary chondrites (Hashizume and Sugiura, 1995).

TABLE 5a. Cosmogenic, radiogenic, fissiogenic and trapped components (in ccSTP/g) in the Sabrum chondrite.

Cosmogenic			Radiogenic			Fissiogenic	Trapped		
^{3}He ($\times 10^{-8}$)	^{21}Ne ($\times 10^{-8}$)	^{38}Ar ($\times 10^{-8}$)	^{4}He ($\times 10^{-8}$)	^{40}Ar ($\times 10^{-8}$)	^{129}Xe ($\times 10^{-12}$)	^{136}Xe ($\times 10^{-12}$)	^{36}Ar ($\times 10^{-8}$)	^{84}Kr ($\times 10^{-12}$)	^{132}Xe ($\times 10^{-12}$)
32.5	8.50	1.057	1209	6057	18.6	0.78	0.38	39.5	43.6

TABLE 5b. Cosmic-ray exposure ages and gas retention ages of the Sabrum chondrite.

Cosmic-ray exposure ages (Ma)			Gas retention ages (Ga)	
T_3	T_{21}	T_{38}	T_4	T_{40}
20.1	24.7	24.9	3.21	4.42

Errors in ages are ±10%.

TABLE 6. Activity of various cosmogenic radioisotopes at the time of fall (1999 April 30) measured in the Sabrum (LL6) chondrite.

Isotope	Half-life	γ-energy (keV)	Sabrum LL6 Counting rate (min^{-1})	Sabrum LL6 Activity (dpm/kg)	Alta'ameen LL5* (1977 August 20) Activity (dpm/kg)	Innisfree LL5* (1977 February 5) Activity (dpm/kg)
^{7}Be	53.29 days	477.56	0.120 ± 0.01	70.0 ± 6.0	–	–
^{58}Co	70.86 days	810.75	0.035 ± 0.01	2.63 ± 0.75	–	–
^{56}Co	77.27 days	846.75	0.056 ± 0.005	4.35 ± 0.40	–	–
^{46}Sc	83.79 days	889.26	0.065 ± 0.005	5.10 ± 0.40	–	9.35 ± 1.3
^{57}Co	271.74 days	122.07	0.068 ± 0.006	3.72 ± 0.33	–	–
^{54}Mn	312.30 days	834.8	0.464 ± 0.004	35.0 ± 0.40	95 ± 19	93.8 ± 3
^{22}Na	2.61 years	1274.54	0.480 ± 0.004	52.8 ± 0.50	101 ± 2	98 ± 2
^{60}Co	5.27 years	1173.20	0.005 ± 0.003	0.64 ± 0.30	<3.8	0.93 ± 0.61
		1332.51	0.007 ± 0.003		–	–
^{26}Al	7.3×10^5 years	1808.65	0.300 ± 0.003	47.1 ± 0.51	62 ± 2	69 ± 1
^{22}Na/^{26}Al	–	–	–	1.12 ± 0.02	1.6	1.4

*Evans *et al.* (1982).

COSMIC-RAY TRACKS AND RADIOACTIVITY

Cosmic-ray tracks and several radionuclides were studied in the Sabrum meteorite. Track density was measured in two diagonally opposite spot samples taken from the basal and subvertical faces. Tracks were revealed after appropriate etching of olivines in WN solution (40% EDTA + 1% oxalic acid and orthophosphoric acid, made to pH 8.0 by adding NaOH; Krishnaswami *et al.*, 1971) for 5 h. Track density was found to be $(1.3 \pm 0.3) \times 10^6$/cm^2, corresponding to shielding depth of 8 ± 1.5 cm if an exposure age of 24.8 Ma is adopted, showing little variation between the two locations.

Cosmogenic radionuclides ^{26}Al, ^{60}Co, ^{22}Na, ^{54}Mn, ^{57}Co, ^{46}Sc, ^{56}Co, ^{58}Co and ^{7}Be were measured in the main mass of the meteorite weighing 461 g, using a 400 cm^3, low-background, high-purity germanium gamma-ray spectrometer located in a 20 cm thick lead shield, described in Shukla *et al.* (2001). Potassium-40 (K = 817 ppm; Table 2) has been used as an internal standard for estimating the activity levels of the cosmogenic radionuclides following the procedure of Bhandari *et al.* (1989). The calculated activities are given in Table 6. We first note that the activity of ^{60}Co (<0.9 dpm/kg), which is mainly produced by capture of thermal neutrons, is low. On comparing it with the calculated production rates as given by Spergel *et al.* (1986), using cobalt concentration of 521 ppm (Table 2), we find that the observed activity of ^{60}Co indicates low thermal neutron fluxes which, in turn, implies low shielding depth and small preatmospheric size (r < 20 cm) of the meteoroid in interplanetary space. Similarly, comparing the observed ^{26}Al activity (47.1 ± 0.5 dpm/kg) with the production depth profiles of ^{26}Al for spherical meteoroids of various sizes (Bhandari *et al.*, 1993; Leya *et al.*, 2000), we estimate that the preatmospheric radius of the Sabrum meteoroid must have been close to ~15 cm.

The activities of short-lived radionuclides can be used to infer the extent of modulation of galactic cosmic rays by sunspot activity. The intensity of galactic cosmic rays is anticorrelated with the sunspot number due to the accompanying changes in the intensity of the heliospheric magnetic field. The neutron monitor count rates, appropriately normalised, enable us to compute the time variation of isotope production rates, if we assume that the isotope production rates are linearly related to the neutron monitor count rates (Bhandari *et al.*, 1989). We have used the Climax neutron monitor data (Solar Geophysical Data, 2000) and numerically integrated the isotope production to obtain their time variation. A small phase lag, relative to the variations in neutron monitor count rates, occurs in activity of radioisotopes with half lives smaller or comparable to the solar cycle, depending on their half life (Evans *et al.*, 1982; Bhandari *et al.*, 1989; Bonino and Castagnoli, 1997) and the long-lived radioisotopes are not at all affected. We compare the observed activities in Sabrum with those measured in Innisfree and Alta'ameen, the other two LL chondrites (Evans *et al.*, 1982), which have similar chemical composition. These meteorites fell in 1977 during the rising phase of solar activity cycle 21, roughly similar to Sabrum, which fell during the rising phase of solar cycle 23. The activities of some of the radionuclides measured in the 1977 falls are also listed in Table 6. We note that the activities of the three radionuclides (^{22}Na, ^{46}Sc and ^{54}Mn), where data are available, are significantly lower in Sabrum (40 to 60%) compared to Innisfree and Alta'ameen. In case of ^{46}Sc and ^{54}Mn, we can compare the activities per kg Fe since it is the main target element. ^{46}Sc (23.3 dpm/kg Fe) and ^{54}Mn (157.8 dpm/kg Fe), both are 40 to 60% lower in Sabrum compared to the 1977 falls. Our results thus indicate that the cosmic-ray fluxes during the rising phase of solar cycle 23 were significantly lower than during solar cycle 21 (Fig. 4). The solar minimum period before solar cycle 21 was quiet and prolonged and the balloon borne detectors (Garcia-Munoz *et al.*, 1977) showed unusually high fluxes.

More significantly, the $^{22}Na/^{26}Al$ ratio in Sabrum (1.12 ± 0.02) is one of the lowest values found in chondrites and is ~25% lower than the expected value. The ratio $^{22}Na/^{26}Al$ is an indicator of the integrated fluxes of cosmic rays during the last 4 to 5 years prior to the fall of the meteorite and such low values are generally found in chondrites, which fall after a solar maximum. About 35 chondrites have been studied for $^{22}Na/^{26}Al$ (Bhandari *et al.*, 1994; Bonino and Castagnoli, 1997; Murty *et al.*, 1998). In Fig. 4, we show the calculated variation based on Climax neutron monitor data (Solar Geophysical Data, 2000), following the procedure of Bhandari *et al.* (1989) for H, L and LL group of meteorites. On average, the H group of chondrites have a value of 1.5 and the L and LL have a value close to 1.35, which varies inversely with the sunspot number with some phase lag, determined by the mean life of ^{22}Na. Most of the chondrites fall within the expected range. Ratios higher than the expected values can arise due to a number of

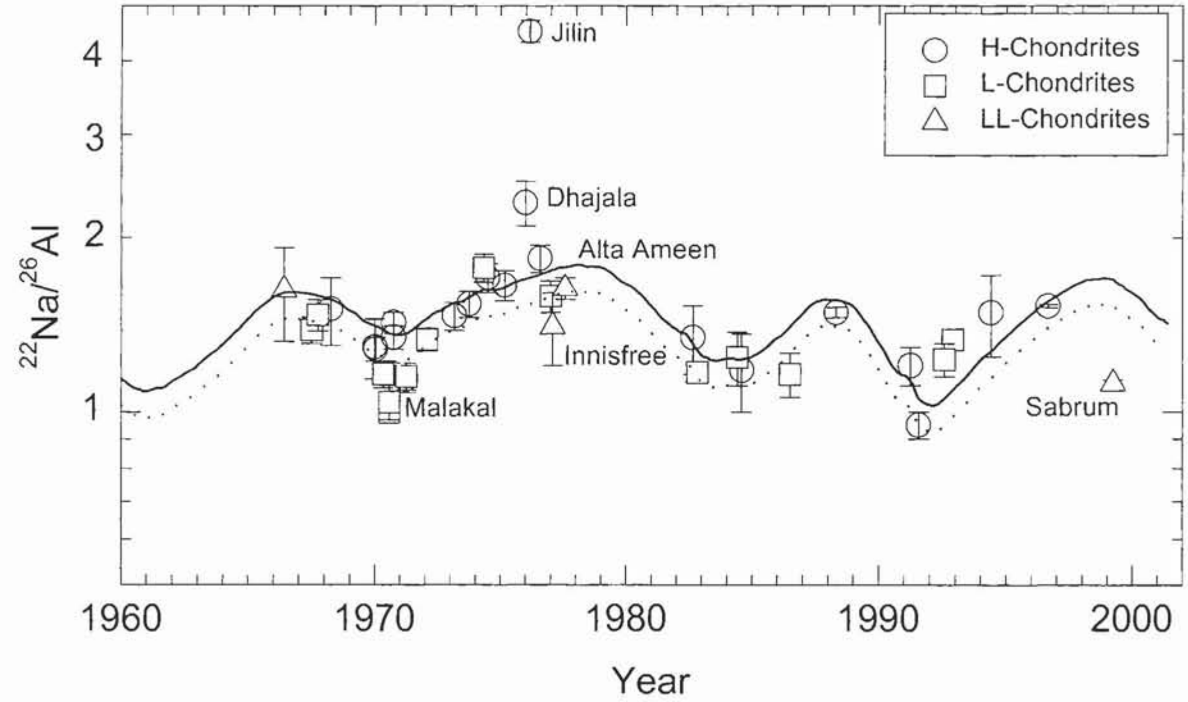

FIG. 4. Solar cycle variation of $^{22}Na/^{26}Al$. The solid curve shows the expected variation based on Climax neutron monitor data for H chondrite (circles). The dotted curve is for L (rectangles) and LL chondrites (triangles). The data are taken from Evans *et al.* (1982), Brown *et al.* (1996), Murty *et al.* (1998), Heusser *et al.* (1985) and Bhandari *et al.* (2002).

reasons (*e.g.*, fragmentation in the interplanetary space, spatial variation of cosmic-ray fluxes over the orbital space of the meteoroid and production by solar flare protons). Fragmentation of a meteoroid in space changes the shielding depth within a meteoroid and consequently the isotope production rates, since nuclear interactions of cosmic rays are depth dependant (see, for example, Leya *et al.*, 2000). When a deep sample containing small or negligible amount of radioactivity, because of low production at large depths, is brought closer to the newly exposed surface, as a result of fragmentation, additional production starts and takes two or three mean lives to attain the secular equilibrium. As a consequence $^{22}Na/^{26}Al$ increases because ^{22}Na quickly attains secular equilibrium whereas ^{26}Al takes a few million years. Fragmentation shortly (0.4 Ma) before the fall of the Jilin meteorite resulted in $^{22}Na/^{26}Al$ ratio in excess of 4 (Heusser *et al.*, 1985). In the case of Dhajala, which had high orbital inclination of ~28° (Bhandari *et al.*, 1978), the observed high ratio of ~2.1 was attributed to heliolatitudinal gradient of cosmic-ray fluxes in interplanetary space.

Ratios lower than the expected values can also arise if the meteoroid is exposed to low cosmic-ray fluxes during the terminal segment of its orbit. There are some meteorites like Malakal which show marginal discrepancy with the expected ratio, probably due to its complex exposure history involving breakup of the meteoroid before the fragment fell on the Earth (Cressy and Rancitelli, 1974). However, there is no indication from rare gas, radioactivity or track data that Sabrum had a complex exposure. Measurements of long-lived radioisotopes (*e.g.*, ^{10}Be and ^{53}Mn) will be useful in understanding the exposure history of this meteorite. Production of ^{26}Al by solar energetic particles (SEP) can also result in low $^{22}Na/^{26}Al$. However, at a shielding depth of 8 ± 1.5 cm, the SEP contribution would be negligible because of their low energy and small penetration depth. Sabrum fell after a solar minimum when the highest $^{22}Na/^{26}Al$ (~1.5) is expected compared to the observed value of 1.12. Therefore, the cosmic-ray fluxes derived from Sabrum data, corresponding to the solar quiet period between cycles 22 and 23 appear to be anomalously low and require further investigation.

In summary, the Sabrum chondrite is classified as an LL6 brecciated veined chondrite based on its petrographic and chemical studies. The exposure age of 24.8 Ma is indicated by cosmogenic components of rare gases. The meteoroid appears to have a radius of ~15 cm, corresponding to a mass of ~50 kg. The radioactivities of short-lived nuclides (<2.6 years) are unusually low and indicate low galactic cosmic-ray fluxes over the orbital space of the meteoroid during the last few years prior to its fall.

Acknowledgements–We thank K. M. Suthar for his help in track analysis and R. Wieler, S. Merchel, U. Herpers, P. Ma, Ian Lyon and R. Jones for useful comments. Our appreciation goes to K. R. Nambiar for his help in preparation of this manuscript. Some of the work reported here was done as a part of the National Planetary Science and Exploration Programme supported by the Indian Space Research Organisation.

Editorial handling: I. C. Lyon

REFERENCES

Bhandari N., Bhattacharya S. K. and Somayajulu B. L. K. (1978) Cosmogenic radioisotopes in the Dhajala chondrite: Implications to variations of cosmic ray fluxes in the interplanetary space. *Earth. Planet. Sci. Lett.* **40**, 194–203.

Bhandari N., Bonino G., Callegari E., Castagnoli G. C., Mathew K. J., Padia J. T. and Queirazza G. (1989) The Torino, H6 meteorite shower. *Meteoritics* **24**, 29–34.

Bhandari N. *et al.* (1993). Depth and size dependence of cosmogenic nuclide production rates in stony meteoroids. *Geochim. Cosmochim. Acta* **57**, 2361–2375.

Bhandari N., Bonino G., Cini Castagnoli G. and Taricco C. (1994) The 11-year solar cycle variation of cosmogenic isotope production rates in chondrites (abstract). *Meteoritics* **29**, 443–444.

Bhandari N., Murty S. V. S., Suthar K. M., Shukla A. D., Ballabh G. M., Sisodia M. S. and Vaya V. K. (1998) The orbit and exposure history of the Piplia Kalan eucrite. *Meteorit. Planet. Sci.* **33**, 455–461.

Bhandari N. *et al.* (2002) Itawa Bhopji (L3/5) chondrite regolith breccia: Fall, classification and cosmogenic records. *Meteorit. Planet. Sci.* **37** (in press).

Bonino G. and Castagnoli G. C. (1997) Solar cycles recorded in meteorites. In *Past and Present Variability of the Solar-Terrestrial System: Measurement, Data Analysis and Theoretical Models* (eds. G. C. Castagnoli and A. Provenzale), p. 491. IOS Press, Amsterdam, The Netherlands.

Bonino G., Bhandari N., Murty S. V. S., Mahajan R. R., Suthar K. M., Shukla A. D., Shukla P. N., Cini Castagnoli G. and Taricco C. (2001) Solar and galactic cosmic-ray records of the Fermo (H) chondrite regolith breccia. *Meteorit. Planet. Sci.* **36**, 831–839.

Brearley A. J. and Jones R. H. (1998) Chondritic meteorites. In *Planetary Materials* (ed. J. J. Papike), pp. 3-1 to 3-398. Reviews in Mineralogy **36**, Mineralogical Society of America, Washington, D.C., USA.

Brown P., Hildebrand A. R., Green D. W. E., Page D., Jacobs C., Revelle D., Tagliaferri E., Wacker J. and Wetmiller B. (1996) The fall of the St-Robert meteorite. *Meteorit. Planet. Sci.* **31**, 502–517.

Cressy P. J. and Rancitelli L. A. (1974) The unique cosmic ray history of the Malakal chondrite. *Earth Planet. Sci. Lett.* **22**, 275–283.

Dasgupta S. P., Sengupta P. R., Dube A., Sengupta N. R. and Dasgupta D. R. (1978). The Dhajala meteorite. *Mineral. Mag.* **42**, 493–497.

Eugster O. (1988) Cosmic ray production rates for ^{3}He, ^{21}Ne, ^{38}Ar, ^{82}Kr and ^{126}Xe in chondrites based on ^{81}Kr-Kr exposure ages. *Geochim. Cosmochim. Acta* **52**, 1649–1662.

Eugster O., Michel J. H., Nidermaan S., Wang D. and Yi W. (1993) The record of cosmogenic, radiogenic, fissiogenic and trapped noble gases in recently recovered Chinese and other chondrites. *Geochim. Cosmochim. Acta* **57**, 1115–1142.

Evans J. C., Reeves J. H., Rancitelli L. A. and Bogard D. D. (1982) Cosmogenic nuclides in recently fallen meteorites: Evidence for galactic cosmic ray variations during the period 1967–1978. *J. Geophys. Res.* **87**, 5577–5591.

Garcia-Munoz M., Mason G. M. and Simpson J. A. (1977) The appearance of superfluxes of quiet time cosmic rays. *15th Int. Cosmic Ray Conf.* **3**, 209.

GHOSH S., PANT N. C., RAO T. K., RAMA MOHANA C., GHOSH J. B., SHOME S., BHANDARI N., SHUKLA A. D. AND SUTHAR K. M. (2000) The Vissannapeta eucrite. *Meteorit. Planet. Sci.* **35**, 913–917.

HASHIZUME K. AND SUGIURA N. (1995) Nitrogen isotopes in bulk ordinary chondrites. *Geochim. Cosmochim. Acta* **59**, 4057–4069.

HEUSSER G., OUYANG Z., KIRSTEN T., HERPERS U. AND ENGLERT P. (1985) Conditions of cosmic ray exposure of the Jilin chondrite. *Earth Planet. Sci. Lett.* **72**, 263–272.

JAROSEWICH E. (1990) Chemical analyses of meteorites: A compilation of stony and iron meteorite analyses. *Meteoritics* **25**, 323–337.

KALLEMEYN G. W., RUBIN A. E., WANG D. AND WASSON J. T. (1989) Ordinary chondrites: Bulk compositions, classification, lithophile-element fractionations, and composition-petrographic type relationships. *Geochim. Cosmochim. Acta* **53**, 2747–2767.

KRISHNASWAMI S., LAL D., PRABHU M. AND TAMHANE A. S. (1971) Olivine: Revelation of tracks of charged particles. *Science* **174**, 287–291.

LAUL J. C. (1979) Neutron activation analysis of geological materials. *Atomic Energy Rev.* **17**, 603–695.

LEYA I., LANGE H-J., NEUMANN S., WIELER R. AND MICHEL R. (2000) The production of cosmogenic nuclides in stony meteoroids by galactic cosmic-ray particles. *Meteorit. Planet. Sci.* **35**, 259–286.

MARTI K. (1967) Trapped xenon and the classification of chondrites. *Earth Planet. Sci. Lett.* **2**, 193–196.

MARTI K. AND GRAF TH. (1992) Cosmic ray exposure history of ordinary chondrites. *Ann. Rev. Earth Planet. Sci.* **20**, 221–243.

MASON B. (1971) *A Handbook of Elemental Abundances in Meteorites*. Gordon and Breach, New York, New York, USA. 555 pp.

MATHEW K. J. AND MURTY S. V. S. (1993) Cosmic ray produced nitrogen in extraterrestrial matter. *Proc. Indian Acad. Sci. (Earth Planet. Sci.)* **102**, 415–437.

MURTY S. V. S., BHANDARI N., SUTHAR K. M., CLEMENT C. J., BONINO G. AND CASTAGNOLI G. C. (1998). Cosmogenic effects in Mbale, L5/6 chondrite. *Meteorit. Planet Sci.* **33**, 1311–1316.

SHUKLA A. D., ADHYARU P. AND BHANDARI N. (2001) Highly sensitive γ-γ coincidence/anticoincidence spectrometer for measurement of low radioactivity in meteorites. In *Proceedings of Symposium on Nuclear Analytical and Radiochemistry* (NUCAR 2001), pp. 554–555. Bhabha Atomic Research Center, Mumbai, India.

SHUKLA A. D., SHUKLA P. N., SUTHAR K. M., BHANDARI N., VAYA V. K., SISODIA M. S., SINHA ROY S., RAO K. N. AND RAJAWAT R. S. (1997) Piplia Kalan eucrite: Fall, petrography and chemical characteristics. *Meteorit. Planet. Sci.* **32**, 611–615.

SOLAR GEOPHYSICAL DATA (2000) National Oceanic and Atmospheric Administration, **674**, Washington, D.C., USA.

SPERGEL M. S., REEDY R. C., LAZARETH O. W., LEVY P. W. AND SLATEST L. A. (1986) Cosmogenic neutron-capture-produced nuclides in stony meteorites. *J. Geophy. Res.* **91D**, 483–494.

STÖFFLER D., KEIL K. AND SCOTT E. R. D. (1991) Shock metamorphism of ordinary chondrites. *Geochim. Cosmochim. Acta* **55**, 3845–3867.

SWINDLE T. D. (1988) Trapped noble gases in meteorites. In *Meteorites and the Early Solar System* (eds. J. F. Kerridge and M. S. Matthews), pp. 535–564. Univ. Arizona Press, Tucson, Arizona, USA.

VAN SCHMUS W. R. AND WOOD J. A. (1967) A chemical-petrologic classification for the chondritic meteorites. *Geochim. Cosmochim. Acta* **31**, 747–765.

WASSON J. T. AND KALLEMEYN G. W. (1988) Compositions of chondrites. *Phil. Trans. R. Soc. London* **A325**, 535–544.